Journal of Cluster Science (2026) 37:93
https://doi.org/10.1007/s10876-026-03044-9

ORIGINAL PAPER

Green Synthesis of *Althaea Officinalis* Extract-Based CuO Nanoparticles and their Biomedical Applications

Elif Kalpar Dogan[1] · Dilek Bahar[2] · Cemile Yilmaz[3] · Sadık Küçükgünay[4] · Fatma Öztürk Küp[5] · F. İnci Özdemir[1]

Received: 21 November 2025 / Accepted: 18 May 2026 / Published online: 17 June 2026
© The Author(s) 2026

Abstract

Althaea officinalis (A. officinalis) contains a rich bioactive composition with high therapeutic potential, primarily consisting of mucilage and phenolic compounds. The composition enables the ecofriendly green synthesis of nanoparticles (NPs) suitable for various biomedical applications by offering high reduction capacity and strong stabilizing properties. We performed the green hydrothermal synthesis of copper oxide nanoparticles (AO@CuO NPs) by using *A. officinalis* extract. The formation of AO@CuO NPs was confirmed by a visible color change, and characteristic absorbance spectrum measured at 484 nm using UV-Vis spectrophotometry. The surface morphologies and charges, chemical and crystal structures, and hydrodynamic diameters of AO@CuO NPs were determined using scanning electron microscopy (SEM), Zeta potential, Fourier-transform infrared spectroscopy (FTIR), and dynamic light scattering (DLS) analyses. The spherical morphology and particle size (30.0 ± 10.0 nm) of AO@CuO NPs were confirmed by SEM analysis. The surface charge value of (-39.7 ± 3.9 mV) obtained by Zeta measurement. It is worth noting that the AO@CuO NPs possessed strong antimicrobial activity and demonstrated the highest inhibitory effect against *P. vulgaris* (18.67 ± 1.15 mm). It was determined that they exhibited moderate antioxidant activity using the DPPH method. Additionally, we detected significant antiproliferative (IC_{50}= 28.3, 10.7, and 253.9 $\mu g.ml^{-1}$) and proapoptotic potentials of AO@CuO NPs on human lung adenocarcinoma (A549), human colorectal (DLD-1) and human hepatocellular carcinoma (HepG2) cancer cells, respectively. Compared to cisplatin (CP), the apoptotic induction capacity in cancer cell lines was confirmed by flow cytometry analysis. Herein, we offer a reliable, sustainable and biocompatible nanotechnology-based biomedical platform approach against resistant infections and cancer. Schematic diagram, presenting the general outline of the research topics.

✉ Fatma Öztürk Küp
fozturk@erciyes.edu.tr

✉ F. İnci Özdemir
i.ozdemir@gtu.edu.tr

1 Department of Molecular Biology and Genetic, Faculty of Science, Gebze Technical University, Kocaeli 41400, Turkey

2 Genkök Genome and Stem Cell Center, Erciyes University, Kayseri 38030, Turkey

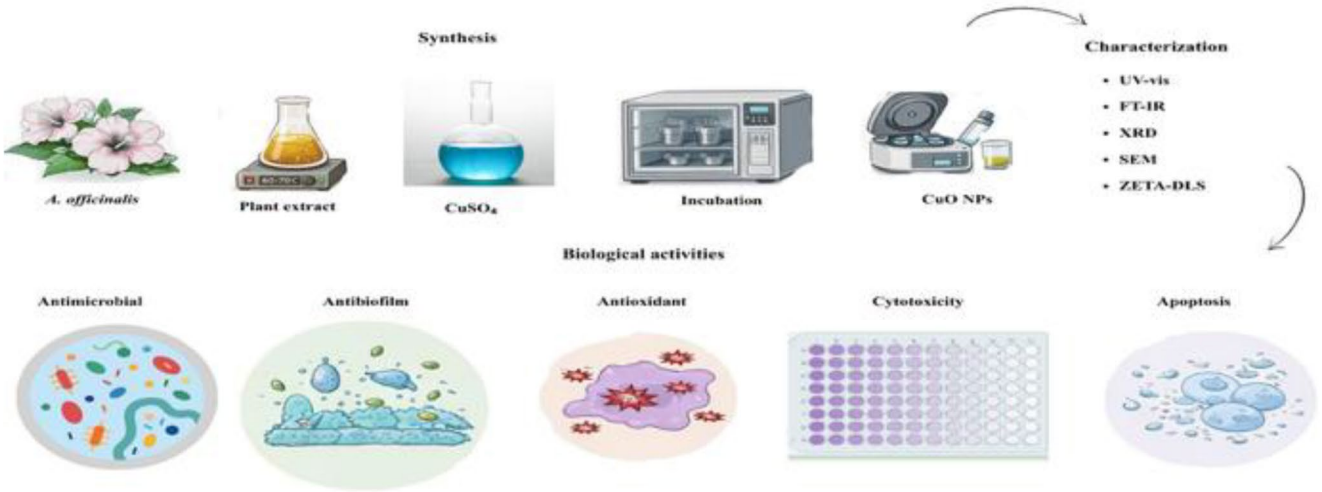
3 Department of Analytical Chemistry, Faculty of Pharmacy, Erciyes University, Kayseri 38280, Turkey

4 Department of Medical Pharmacology, Faculty of Medicine, Kırşehir Ahi Evran University, Kırsehir 40100, Turkey

5 Department of Biology, Faculty of Science, Erciyes University, Kayseri 38039, Turkey

Graphical Abstract

Schematic diagram, presenting the general outline of the research topics



Keywords Antimicrobial activity · *Althaea officinalis* · Antibiofilm activity · Copper oxide nanoparticles · Cytotoxicity

Introduction

Green nanotechnology uses sustainable resources such as biological agents and cellular components instead of toxic chemicals. Compared to conventional synthesis methods, it is ecofriendly, easy to produce, and inexpensive. Plants, bacteria, fungi, yeasts and actinomycetes are sources of biological material. Among these, plant materials are frequently preferred due to their rich phytochemical contents, as well as their stabilizing and reducing capacities [1, 2]. *Althaea officinalis* (*A. officinalis*), also called marshmallow, is a native plant of the Malvaceae family, native to Asia, Europe and the United States [3]. This plant contains important compounds such as coumarins, pectin, mucilage, phytosterols, starch, mono- and disaccharides, flavonoids, scopoletin, tannins, asparagine and many amino acids. It is widely used in the treatment of conditions such as inflammation, ulcers, skin burns and irritation of the pharyngeal mucosa [4, 5]. Also, the cytotoxic activity of this plant has been supported by several studies, linked to its composition of coumarins, phenolic acids, and flavonoids [6]. B-glucans forming mucilage structure of the plant, were suggested as adjuvants to enhance the efficacy of immunotherapy and chemotherapy [7]. β-glucans exhibit anti-tumor activity by increasing neutrophil activation and reducing lung metastasis [8]. In addition, the diverse chemical components of *A. officinalis* help to explain pharmacological properties such as antibacterial, antitussive, anti-inflammatory, antioxidant and antifungal effects [9, 10]. Due to these properties, *A. officinalis* extract is widely used in the green synthesis of metallic NPs such as, primarily silver nanoparticles (Ag NPs) [11–13] and zinc oxide nanoparticles (ZnO NPs) [14].

Copper (Cu) is widely used due to unique physical and chemical properties [15]. As a transition metal, Cu acts as a catalyst in Haber-Weiss and Fenton-like reactions. There is a continuous exchange of electrons between Cu^{+} and Cu^{2+} ions. In this process, increased the reactive oxygen species (ROS) levels trigger oxidative stress [16]. These radical species occur in a series of complex chemical reactions, leading to enzyme imbalance, lipid peroxidation, damage to proteins and nucleic acids, impair organ function, and ultimately cell death [17]. Specifically, copper oxide nanoparticles (CuO NPs) are classified as metal oxide group nanostructures with antimicrobial, catalytic activity and low production costs. CuO NPs exhibit superior thermal, magnetic, and mechanical properties, as well as a high surface area/volume capacity [18, 19]. Their nanoscale dimensions enable effective interaction at the cellular level, similar to biomolecules such as enzymes and receptors. Their specific interactions and suitable morphological structures enable them to actively participate in the early diagnosis and targeted treatment of cancer [20, 21]. The cytotoxic mechanisms of CuO NPs are primarily based on triggering apoptosis by interacting with intracellular macromolecules and causing cellular leakage and cell death due to membrane disruption [22, 23]. CuO NPs, which are notable for their superior physical, biochemical, and pharmacological properties, have been obtained through green synthesis using various plant materials such as *Amomum subulatum* [24], *Macroptilium Lathyroides* [25], pumpkin seed [26] and *Tecoma stans* leaf [27].

In previous studies, *A. officinalis* extract has been used in the synthesis of Ag and ZnO nanoparticles; however, it has not been previously reported for the synthesis of CuO NPs. Until now, no comprehensive study has evaluated the antimicrobial and antibiofilm effects of plant-derived CuO NPs alongside the mechanisms of cellular apoptosis and cytotoxicity. In this study, we report the synthesis of AO@CuO NPs via a green hydrothermal method using *A. officinalis* extract, which has a dual effect as a stabilizer and reducing agent. The antimicrobial and antibiofilm activities of AO@CuO NPs against various Gram-positive, Gram-negative bacteria, and fungi, as well as their antioxidant capacities, were also identified. The cytotoxicity and apoptosis effects were assessed in against human lung adenocarcinoma (A549), human hepatocellular carcinoma (HepG2), human colorectal carcinoma (DLD-1), and mouse fibroblasts (L929) cell lines using the MTT assay and Muse® Annexin V & Dead Cell Kit to fill the critical research gap. Their activities were profiled by comparing them with the standard reference drug, cisplatin (CP). Ultimately, based on the versatile findings obtained in the activity studies of AO@CuO NPs, it is predicted that these nanostructures will constitute an eco-friendly and effective alternative for biomedical applications.

Materials and Methods

Materials

Analytically pure components: copper II sulphate ($CuSO_4$), sodium hydroxide (NaOH), ampicillin, cisplatin, crystal violet, 3-[4,5-dimethylthiazol-2-yl]−2,5-diphenyltetrazolium bromide (MTT), and the microbiological culture media, namely Mueller-Hinton Broth (MHB) and Nutrient Broth (NB) and complete media for cell culture (DMEM High Glucose, Ham's F-12, RPMI-1640 and F-12 K) were supplied from Sigma-Aldrich. Plant material, *A. officinalis* flowers, was purchased in dried form from Saraçoğlu Company (Turkey). Different model microorganisms used in microbiological investigation: *Staphylococcus aureus (S. aureus)*, *Proteus vulgaris (P. vulgaris)*, *Enterobacter aerogenes (E. aerogenes)*, *Bacillus subtilis (B. subtilis)*, *Escherichia coli (E. coli)*, *Staphylococcus epidermidis (S. epidermidis)* bacteria, and *Candida albicans (C. albicans)* and *Candida parapsilosis (C. parapsilosis)* yeasts were obtained from the culture collection stocks of the Biology Department at Erciyes University. The Muse® Annexin V & Dead Cell kit were procured from Cytek. The cell lines (A549, HepG2, DLD-1 and L929) were provided from the Genome and Stem Cell Centre (GENKOK) at Erciyes University.

Preparation of Plant Material and Aqueous Extract

In the plant extraction process, *A. officinalis* (2 g), which had been powdered using a grinding device, was weighed and transferred into 100 mL of distilled water. The mixture was subjected to thermal processing at 60 °C for 1 h (h) to ensure the solubility of the components. Subsequently, coarse residues were removed using Whatman No. 1 filter paper. The resulting filtrate was centrifuged at 5000 rpm for approximately 10 min (min) to remove particulate impurities. The clear phase (supernatant) was decanted and stored at +4 °C for subsequent biosynthesis stage [28].

Biosynthesis and Characterization of AO@CuO NPs

A green hydrothermal method was selected to produce AO@CuO NPs using an environmentally friendly approach. In the synthesis process, *A. officinalis* extract was added dropwise to a 20 mM $CuSO_4$ solution (50 mL) in equal volume ratio (1:1, v/v) and mixed. The reaction medium was adjusted to pH 11 and vortexed for 30 s to achieve homogenisation. It was subsequently placed in a Teflon-lined hydrothermal autoclave and heat-treated at 120 °C for 5 h. At the end of incubation, the formation was confirmed by a color change (from yellow to brown) reaction, and the liquid was subjected to centrifugation at 10,000 rpm for 10 min to separate the precipitate. The product was washed twice with distilled water to remove undesirable organic residues, dried at 40 °C in the final stage, and stored at +4 °C for subsequent use [29].

Initially, the absorption spectra of *A. officinalis* extract and AO@CuO NPs were measured using UV-Vis spectrophotometry (UV1900i; Shimadzu, Japan). The surface morphologies and average particle sizes by scanning electron microscopy (SEM, ZEISS EVO LS10), the chemical structures by the FT-IR spectrometer (Perkin Elmer, 400 FT-IR Spectrometer Spotlight 400 Imaging System), and the crystallographic structure by X-ray diffraction (XRD, Bruker AXS D8) were characterized of NPs. The stability of NPs is evaluated by determining their hydrodynamic diameters and surface charges using dynamic light scattering (DLS, Malvern, Nano ZS90) and Zeta potential (Malvern, Nano ZS90), respectively.

Antimicrobial Activity of *A. Officinalis* and AO@CuO NPs

Agar Well Diffusion

The antimicrobial activities of *(A) officinalis* extract and AO@CuO NPs were tested using agar well diffusion

method with a modified approach [30]. The test was performed against *S. aureus*, *E. aerogenes*, *S. epidermidis*, *(B) subtilis*, *P. vulgaris*, *E. coli* bacterial strains and *(C) albicans*, *C. parapsilosis* yeast strains. After being revived in the mid-log phase, the bacterial and yeast cultures were spread on Muller Hinton agar (MHA) and Sabourod Dextrose agar (SDA), respectively. Subsequently, 6 mm diameter wells were created in the petri dishes. AO@CuO NPs (1000 µg/mL) and *A. officinalis* extract (2%, w/v) were supplemented into the respective well. Ampicillin and fluconazole from positive control groups were used at concentrations of 10 µg/disc and 25 µg/disc for bacteria and yeasts, respectively. Bacteria were incubated at 37 °C for 24 h, while yeasts were incubated at 25 °C for 48 h. The inhibition zone diameter (mm) was recorded at the end of the incubation periods and evaluated by comparison with the control groups.

Assessment of Minimum Inhibitory (MIC) and Bactericidal/Fungicidal Concentration (MBC/MFC)

The inhibitory effects of synthesized AO@CuO NPs on model microorganisms were analyzed using the broth microdilution technique in 96-well sterile microplates. AO@CuO NPs were subjected to a two-fold serial dilution process in the concentration range of 1000 to 0.075 µg/mL. Each well containing these concentrations was incubated under the previously specified conditions after adding 100 µL of standardized bacterial and yeast suspensions. The lowest AO@CuO NP concentration at which microbial growth could not be detected by the naked eye was recorded as the MIC value. Sterile medium without microorganisms was employed as the negative control in the experiment, while medium without NP but with added microorganisms was employed as the positive control. To determine the MBC/MFC, samples taken from the non-turbid wells were inoculated onto MHA and SDA, respectively. The lowest AO@CuO NP concentration at which no colony formation was observed on the agar surface at the end of the incubation period was defined as the MBC and MFC values, respectively [31, 32].

Effect of AO@CuO NPs on Biofilm Formation

For the biofilm inhibition assessment, *E. coli*, *E. aerogenes*, and *S. aureus* strains were selected. Bacterial suspensions were incubated in MHB until they reached the 0.5 McFarland standard and were transferred to 96-well microplates [33]. AO@CuO NPs prepared in a concentration range of 125 µg/mL to 1000 µg/mL were applied to these plates and incubated at 37 °C for 48 h. Wells containing only the medium without AO@CuO NPs were designated as the negative control group. Following the incubation period, the plates were washed three times with distilled water and stained with 0.1% crystal violet for 20 min to each well. Excess dye was removed, and the dye bound to the biofilm layer was solubilized with 96% ethanol. Finally, the optical densities of samples at 590 nm were measured using an ELISA microplate reader [34].

The biofilm inhibition (%) of the positive control and AO@CuO NPs was determined using the following formula Eq. (1):

$$Biofilm\ inhibition\ (\%) = \left[\frac{Acontrol\ -\ Asample}{A\ control}\right] \times\ 100 \qquad (1)$$

Antioxidant Activity Assay of AO@CuO NPs

The free radical scavenging activity of AO@CuO NPs was determined using the 2,2-diphenyl-1-picrylhydrazyl (DPPH) assay [35]. 1 mL methanolic DPPH (0.1 mM) solution was mixed with different concentrations (200, 100, 50, 25 and 12.5 µg/mL) of 0.5 mL AO@CuO NPs and *A. officinalis* extract. Following the incubation of the mixtures in the dark at room temperature (RT: 25 °C) for approximately 20 min, their absorbances were measured at 517 nm. Methanol was selected as the negative control, while butylated hydroxytoluene (BHT) was selected as the positive control [36].

The percentage of scavenging activity (%) was measured using the following formula Eq. (2):

$$DPPH\ inhibition\ (\%) = \left[\frac{Acontrol\ -\ Asample}{A\ control}\right] \times\ 100 \qquad (2)$$

Cell Culture Assay

Evaluation of Cytotoxicity

The in vitro cytotoxicity of *A. officinalis* and AO@CuO NPs was determined using the MTT cell viability assay onto DLD-1, A549, HepG2, and L929 cell lines. All tested cells were treated with different concentrations (250, 125, 62.5, 31.25, 15.625 µg/mL) of *A. officinalis* extract and AO@CuO NPs. Cell viability was determined by the formation blue-coloured formazan salt following the reduction of MTT dye by the mitochondrial enzyme succinate-dehydrogenase [37]. Firstly, DLD-1 cells were cultured in DMEM High Glucose, A549 cells in Ham's F-12, HepG2 cells in RPMI-1640, and L929 cells in F-12 K medium, each supplemented with 10% fetal bovine serum (FBS) and 1% penicillin–streptomycin. All cells maintained at 37 °C in a humidified atmosphere containing 5% CO_2. Cells with appropriate confluency were inoculated into 96-well plates at a density of 5000 cells/

mL (100 µL/well) and incubated for 24 h at 37 °C under a 5% CO_2 atmosphere. Subsequently, the cells were washed with fresh medium, and the adherent cells were treated with AO@CuO NPs and *A. officinalis* extract at concentrations ranging from 0 to 250 µg/mL. After incubation for 48 h at 37 °C in a 5% CO_2 atmosphere, the cells were washed twice with phosphate-buffered saline (PBS). 100 µL of MTT reagent (5.0 mg/mL) was added to each well and incubated in the dark for 3 h at the same condition. Thus, MTT was converted to insoluble formazan crystal by metabolically active cells. After the cell medium was aspirated, formed formazan crystals were dissolved with 100 µL of dimethyl sulfoxide (DMSO). Untreated cells and CP were used as negative and positive control, respectively. The absorbance of microplates was measured at 560 nm using a microplate reader (Promega Glomax). The half maximal inhibitory concentration (IC_{50}) was calculated for each cell type separately using dose–response curves [13]. The cell viability (%) was determined using following formula Eq. (3):

$$Cell\ viability\ (\%) = \left[\frac{A\ sample}{A\ control}\right] \times\ 100 \tag{3}$$

Flow Cytometry Assay for Apoptotic Cells

The effect of *A. officinalis* extract and AO@CuO NPs on apoptosis/dead cells was determined using flow cytometry. DLD-1, A549, HepG2 and L929 cells were seeded independently into 24-well plates at 2×10^4 cells/mL and incubated for 24 h at 37 °C in a humidified atmosphere containing 5% CO_2. Cells were treated with IC_{50} of AO@CuO NPs at 37 °C for 48 h. Untreated and CP-treated cells were used as a negative and positive control, respectively. After the medium was aspirated, cells were harvested by 200 µL of trypsin to remove the cells from the surface. The cell suspension was centrifuged at 350 × g for 5 min and washed at least twice with PBS. The apoptotic cell populations were analyzed using the Muse® Annexin V & Dead Cell Kit (MCH100105) according to the manufacturer's instructions. 50 µL Muse® Annexin V & Dead Cell reagent was added to 50 µL cells. The tested cells were incubated for 20 min in the dark at room temperature. The percentage of apoptotic/dead cells was evaluated using flow cytometry (FACSAriaIII) [38]. The obtained data were evaluated using FlowJo software (Version 7.6.1) to determine the percentage of viable, early apoptotic, late apoptotic and necrosis cells.

Statistical Analysis

All experiments were repeated in triplicate. The data are shown as mean ± standard error and plotted to each graph. Unpaired T-test analysis was performed to compare the treatment groups (*$P<0.05$, **$P<0.01$, ***$P<0.001$).

Results and Discussion

Green Synthesis of AO@CuO NPs by Using *A. Officinalis* Extract

In this study, AO@CuO NPs were successfully synthesized using the hydrothermal synthesis method with *A. officinalis* aqueous extract. The extract was used as both a stabilizing and reducing agent, as it contains rich phytochemical content. The biosynthesis of AO@CuO NPs was initially determined by the color change observed at the end of the reaction (from yellow to dark brown), as well as by UV-vis spectroscopy (Fig. 1a and b). The UV-Vis spectrum showed an absorption peak at 322 nm for the *A. officinalis* extract and 484 nm for the AO@CuO NPs. [39, 40].

The SEM analysis shown in Fig. 1c confirms that AO@CuO NPs aggregate through supramolecular assembly, forming regular shapes. These formations may be related to particle clustering due to the self-assembly effect. According to the report by Zak and colleagues [41], as the particle size decreases, the ratio of surface atoms to all atoms within the particle increases, thereby affecting the particle morphology. In addition, it can be said that the rich mucilage content of *A. officinalis* also affects the formation [10]. Studies conducted with *Abelmoschus esculentus* fruit extract [42] and *Aloe vera* extract [43] have determined that the mucilage structure leads to supramolecular structure. According to SEM analysis, AO@CuO NPs were found to have a particle size of 30 ± 10 nm and a spherical structure. The hydrodynamic diameters were determined as 705.2 nm (Fig. 1d) via DLS. The surface charge densities were recorded as −39.7 ± 3.9 mV via the Zeta potential and the PDI value of AO@CuO NPs was 0.5 (Fig. 1e). The high negative charge of AO@CuO NPs ensures high stability to the NPs due to electrostatic repulsion force [44]. The highly negatively or positively charged NPs are quite stable and colloidal in solution. Regarding the DLS spectrum, while hydrodynamic size of NPs is much bigger than the size of NPs measured in SEM image, hydrodynamic size gives a very mono-dispersed and narrow size distribution in Fig. 1d, which is consistent with the stability of NPs. The large size of NPs in DLS measurement can be attributed to electrical double layer (EDL) theory. The EDL occurs on the surface of NPs prepared in solution form. The AO@CuO NPs are highly negatively charged in solution, the positive charge side of solvent molecules appears on the surface of AO@CuO NPs, then the negative charge side of solvent molecules covers positive charges for neutralization [45, 46].

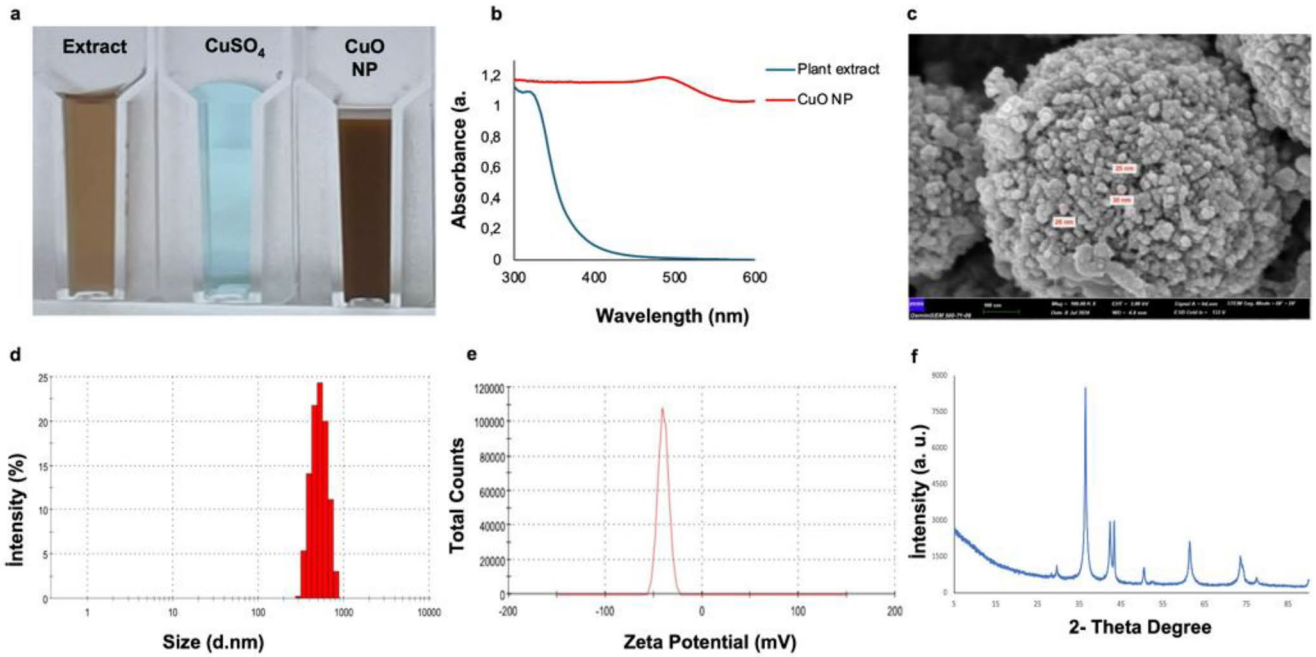


Fig. 1 Characterization of AO@CuO NPs. (**a**) Color changes, (**b**) UV-Vis absorption spectra, (**c**) FE-SEM image, (**d**) DLS spectra, (**e**) Zeta Potential and (f) XRD diffraction pattern

The EDL covers the surface of AO@CuO NPs, then much high effective diameters are measured by DLS.

The crystal structure and sizes of AO@CuO NPs were examined by XRD analysis (Fig. 1f). AO@CuO NPs were scanned at 2θ in the range of 5 to 90 degrees, consistent with JCPDS 85–1326 and JCPDS 77–0199 cards [47, 48]. The diffraction peaks observed at 2θ = 29.62°, 36.44°, 42.35°, 61.39° and 73.58° corresponded to the (110), (111), (200), (220), and (311) crystal planes, respectively. The planes were in line with the JCPDS 85–1326 card. The values of 2θ = 43.32°, 50.49°corresponding to the (111), and (200) planes, were found to be consistent with the JCPDS 77–0199. The values confirmed the formation of CuO NPs containing copper II oxide and copper metal phases. The crystallite sizes of AO@CuO NPs were on average 24 nm, and this value was computed using the Debye-Scherrer equation. The formula: [49]

$$D = \frac{0.9\lambda}{\beta \cos\theta}$$

As shown in Fig. 2, FT-IR spectra in the 4000–400 cm^{-1} range characterized the functional groups and structural changes of *A. officinalis* and synthesized AO@CuO NPs. In the analysis of the *A. officinalis* extract shown in Fig. 2a, the broad band at 3193 cm^{-1} and the band at 2902 cm^{-1} indicate the stretching vibrations of O-H and aliphatic C-H groups, respectively. The sharp bands at 1595 cm^{-1} can be attributed to C=O and C-O stretching vibrations, and the band at 1398 cm^{-1} corresponds to aromatic C-H bending vibrations. The structure of AO@CuO NPs was investigated through changes in the characteristic peaks of potential functional groups (Fig. 2b). The bands corresponding to the O-H and aliphatic C-H group stretching vibrations were observed at 3379 cm^{-1} and 2927 cm^{-1}, whereas the bands of the C=O group were observed at 1589 cm^{-1} and those of the C-O groups at 1368 cm^{-1}. These shifts indicate that these groups are responsible for the reducing and stabilizing effects of AO@CuO NPs. Furthermore, the band identified at 1095 cm^{-1} in the structure of AO@CuO NPs is attributed to C-O-C stretching vibrations and indicates the presence of phytochemical components derived from *A. officinalis* on the surface of the NPs [36, 50]. In the fingerprint region, the characteristic band identified at 605 cm^{-1} corresponds to Cu-O stretching vibrations and confirms the formation of CuO NPs [51]. FT-IR peaks and their corresponding functional groups are shown in Table 1.

Agar Well Diffusion Method

The antimicrobial activity of AO@CuO NPs (1000 µg/mL) and *A. officinalis* extracts (2%, w/v) was determined against test strains using the agar well diffusion method. Standard antibiotic discs (ampicillin 10 µg/disc, fluconazole 25 µg/disc) were used as controls. As shown in Fig. 3; Table 2, while single *A. officinalis* extract did not produce any inhibition zones, the diameters of the inhibition zones produced by AO@CuO NPs were found to range from 11.67 ± 0.58 and 18.67 ± 1.15 mm. In addition, the ampicillin and fluconazole

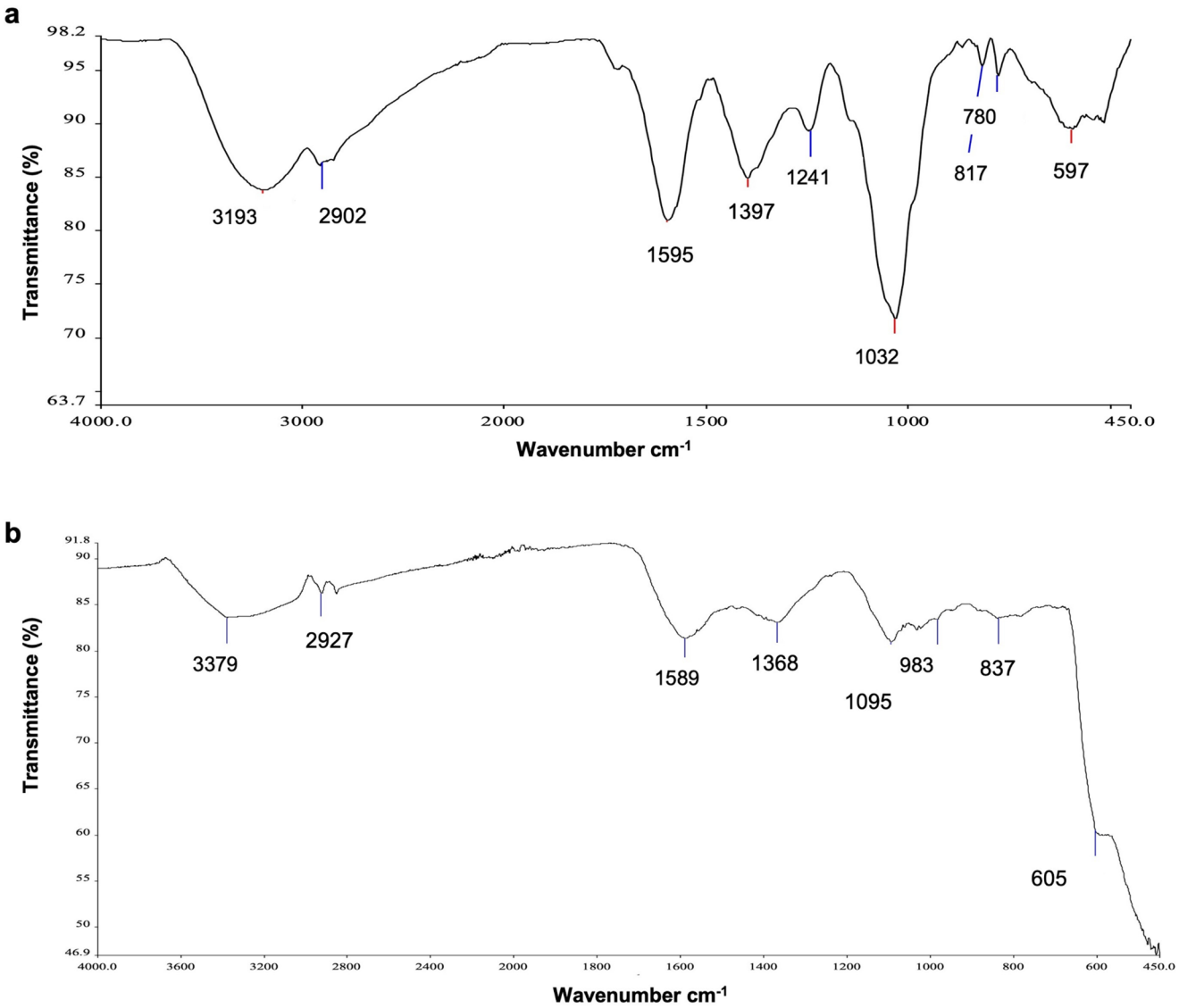


Fig. 2 FT-IR spectra of (**a**) *A. officinalis* extract and (**b**) AO@CuO NPs

Table 1 Functional groups of *A. officinalis* contribute to stabilization of AO@CuO NPs

FT-IR Intensity (cm^{-1})	Class	Functional Group
3193–3379	Alcohol	O-H
2902–2927	Alkanes	C-H
1589–1595	Amide	C=O
1368–1397	Alkane/Phenol	C-H/O-H
1032–1095	Ether	C-O-C
597–605	Metal Oxide	Cu-O

standard drug groups showed high inhibition zone diameters ranging from 10.25±0.58 to 25.67±0.58 mm, and according to this, the activity of the obtained AO@CuO NPs is promising. It has been observed that the phytochemical components in the *(A) officinalis* content not only synthesize NPs but also impart antimicrobial properties to them. Specifically, the lowest zone diameter was measured in the *S. aureus* (Gram-positive) and the highest in the *P. vulgaris* (Gram-negative). This condition can be clarified by the difference in cell membrane structure. Interaction between NPs and a large surface area of a microbial cell compromises membrane integrity. This disruption leads to leakage of bacterial cytoplasmic contents and antimicrobial activity [52]. Similarly, Riazunnisa and colleagues [53] report that *Pithecellobium dulce*-mediated copper oxide nanoparticles (CuO NPs) exhibited the highest antibacterial activity against *E. coli* (15.57±0.5 mm) and the lowest against *(B) subtilis* (10.5±0.5 mm).

Determination of MIC and MBC/MFC

MIC and MBC values of AO@CuO NPs were determined toward the microorganisms listed in Table 3. Among the

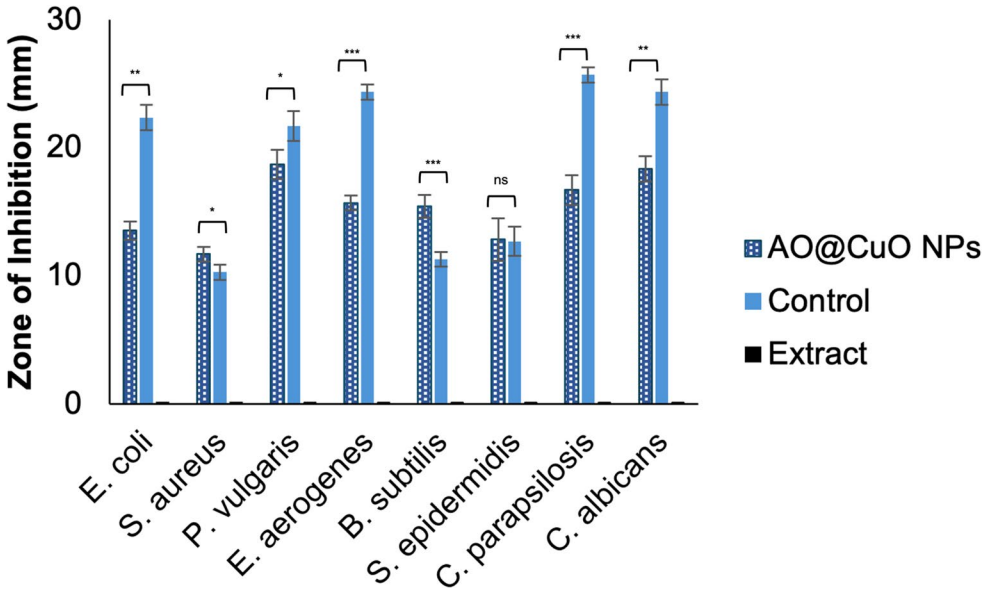


Fig. 3 Antimicrobial activity of extract, AO@CuO NPs and control. *A. officinalis* extract expressed in black indicates a zero level of antimicrobial activity, as it did not demonstrate any efficacy. *$P<0.05$, **$P<0.01$, ***$P<0.001$ compared to control (antibiotics)

Table 2 Summary of inhibition zone of AO@CuO NPs. *$P<0.05$, **$P<0.01$, ***$P<0.001$ compared to control (antibiotics)

Microorganisms	AO@CuO NPs (mm)	Control (mm)	Extract (mm)
E. coli	$13.50\pm0.71^{**}$	22.33 ± 1.53	0
S. aureus	$11.67\pm0.58^{*}$	10.25 ± 0.58	0
P. vulgaris	$18.67\pm1.15^{*}$	21.67 ± 1.15	0
E. aerogenes	$15.67\pm0.58^{***}$	24.33 ± 0.58	0
B. subtilis	$15.40\pm0.89^{***}$	11.25 ± 0.58	0
S. epidermidis	12.80 ± 1.64^{ns}	12.67 ± 1.15	0
C. parapsilosis	$16.67\pm1.15^{***}$	25.67 ± 0.58	0
C. albicans	$18.33\pm1.53^{**}$	24.33 ± 1.15	0

Table 3 MIC and MBC results (µg/mL) of AO@CuO NPs

Bacterial isolates	MIC	MBC	MBC/MIC
S. aureus	250	500	2
P. vulgaris	125	125	1
E. aerogenes	125	500	2
B. subtilis	250	250	1
E. coli	62	125	2
S. epidermidis	125	500	2
Fungal isolates	**MIC**	**MFC**	**MFC/MIC**
C. parapsilosis	15	250	16
C. albicans	31	250	8

tested microorganisms, the lowest MIC of AO@CuO NPs was observed with *E. coli* (62 µg/mL) from bacteria and with *C. parapsilosis* (15 µg/mL) from fungus compared to others. The obtained values are compatible with the current literature indicating that bacteria with high cell wall content exhibit higher resistance to AO@CuO NPs [25]. Additionally, the MIC values measured against *C. albicans* and *C. parapsilosis*, at 31 µg/mL and 15 µg/mL, respectively, are consistent with studies in the literature. Padmavathi and colleagues [54] declared that CuO and Cu_2O NPs destroyed the cell membrane by inhibiting ergosterol production, leading to a loss of virulence. Therefore, high fungal inhibitory activity was observed even at low concentrations. AO@CuO NPs were determined to have a significant inhibitory effect on all tested pathogens.

Antibiofilm Activity of AO@CuO NPs

NPs used as antibacterial agents are expected to penetrate microbial cells and prevent biofilm formation [55]. *S. aureus*, *E. coli*, and *E. aerogenes* are pathogenic bacteria commonly found in human and animal habitats. In this study, the antibiofilm activity of AO@CuO NPs was evaluated on these three bacteria and the results are shown in Fig. 4. AO@CuO NPs at concentrations of 1000, 500, 250, and 125 µg/mL were applied to biofilm-forming bacterial cells, and the results were compared with a 100 µg/mL ampicillin used as a positive control group. When the data were compared with ampicillin, it was seen that AO@CuO NPs inhibited biofilm formation on cells more effectively at all concentrations above 250 µg/mL (Table 4). The highest inhibitory rates of NPs at concentrations of 1000 µg/mL on *S. aureus*, *E. coli*, and *E. aerogenes* were determined as 82.5%, 85.1%, and 98.6%, respectively. Gram-negative *E. coli* and *E. aerogenes* are structurally different from *S. aureus*, a Gram-positive bacterium. The low inhibitory effect of AO@CuO

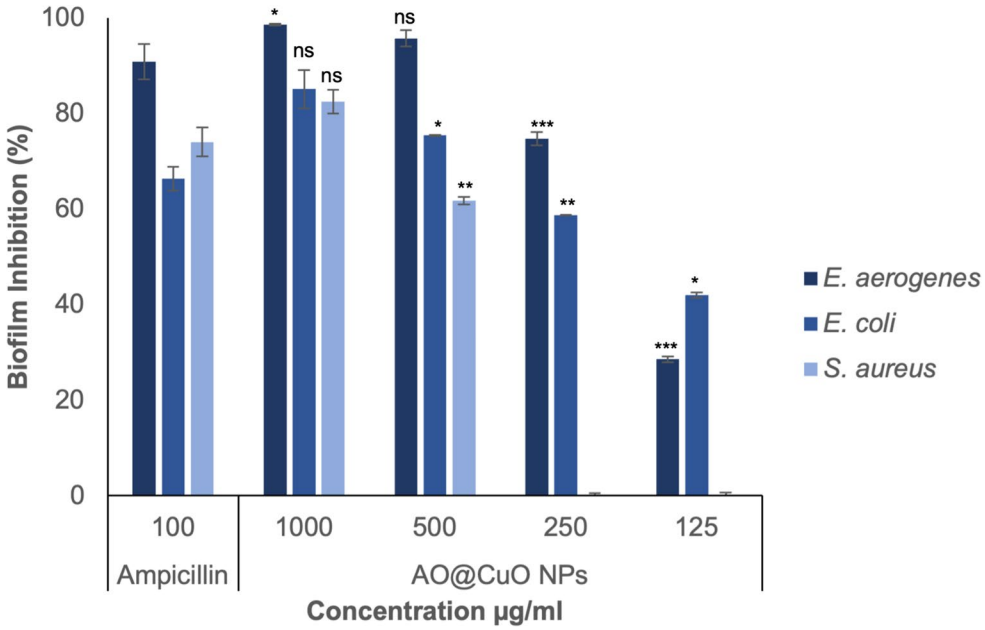


Fig. 4 Effect of AO@CuO NPs on biofilm production. $*P<0.05$, $**P<0.01$, $***P<0.001$ compared to control (antibiotics)

Table 4 Percentage (%) inhibition of biofilm by AO@CuO NPs and ampicillin, *ND* Not detected (no measurable biofilm inhibition). $*P<0.05$, $**P<0.01$, $***P<0.001$ compared to control (antibiotics)

	Concentration (µg/mL)	Biofilm İnhibition (%)		
		Bacterial isolates		
		E. aerogenes	E. coli	S. aureus
Ampicillin	100	90.8±3.6	66.3±3.0	74.0±2.5
AO@CuO NPs	1000	$98.6\pm0.2^{*}$	85.1 ± 2.6^{ns}	82.5 ± 3.8^{ns}
	500	95.7 ± 1.7^{ns}	$75.4\pm0.8^{*}$	$61.7\pm0.6^{**}$
	250	$74.7\pm1.3^{***}$	$58.7\pm0.5^{**}$	ND
	125	$28.6\pm0.6^{***}$	$42.0\pm0.6^{*}$	ND

NPs on Gram-positive *S. aureus* is likely due to presence of teichoic acid in the cell wall, which supports strong biofilm formation [56]. The other reason for the lower effect on gram positive bacteria can be clarified by the polysaccharide intercellular adhesin (PAI) structure which allows bacteria to adhere tightly to cell surfaces [57]. All these results suggest that AO@CuO NPs can penetrate the biofilm matrix, insert bacterial cells, and cause membrane disruption. Our results are consistent with those of Khairy and colleagues [35] who indicated that CuO NPs synthesized using Jojoba extract reduced bacterial adhesion by 90.2–95.0% and 87.2–93.7%, respectively, at 125–62.5 µg/mL. Similarly, CuO NPs synthesized with Neem extract decreased bacterial adhesion by 90.2–95.0% and 87.2–93.7%, respectively, at 125–62.5 µg/mL. Additionally, they showed that the difference in biofilm inhibition is associated with the material's size, antimicrobial activity and penetration ability.

Evaluation of Free Radical Scavenging Activity

Antioxidants neutralize free radicals by fighting reactive oxygen species and play a role in the prevention and therapy of diseases. The antioxidant activity of NPs is strongly influenced by several physicochemical characteristics, including their chemical composition, surface charge, particle size, surface-to-volume ratio and surface coating [58]. *A. officinalis* extract and AO@CuO NPs at various concentrations (200, 100, 50, 25 and 12.5 µg/mL) was estimated using the DPPH free radical scavenging assay. BHT was used as a positive control. The IC_{50} values of AO@CuO NPs, *A. officinalis* extract and BHT were determined as approximately 70.6, 45.0 and 12.0 µg/mL, respectively. AO@CuO NPs exhibited 73.0-19.1% for the various concentrations (12.5–200 µg/mL). The highest inhibition value was determined as 74.6% with *A. officinalis* extract. *A. officinalis* showed higher antioxidant activity than the AO@CuO NPs. This may be due to the high amount of phenolic and flavonoid compounds in plant extract. These metabolites show antioxidant behaviour and act as electron and hydrogen donors in radical scavenging reactions [59]. Both samples showed only modest dose-dependent increase in antioxidant activity (Fig. 5; Table 5). Consistent with our results, Azharuddin and colleagues [60] found that *Arthospira platensis* derived CuO NPs showed strongest inhibition, reaching approximately 69% at 125 µg/mL. Narayana and colleagues [61] performed the biosynthesis of PO-Cu NPs using the extract of *Pleurotus ostreatus* (PO). The antioxidant activity of PO-Cu NPs was determined to be approximately 78% at 150 µg/mL, which is consistent with our results.

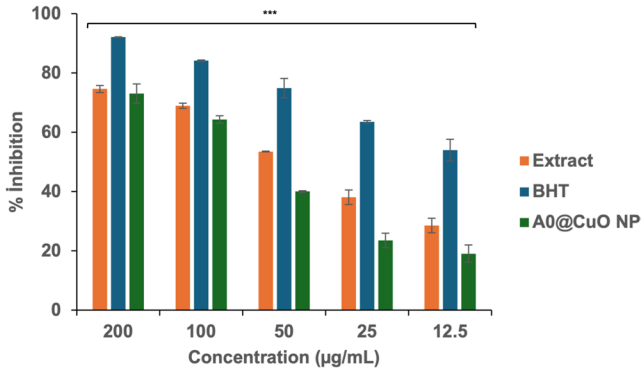


Fig. 5 Free radical scavenging activity of AO@CuO NPs, *A. officinalis* extract and BHT. *$P<0.05$, **$P<0.01$, ***$P<0.001$ compared to BHT

Table 5 Percentage (%) DPPH-scavenging activity of AO@CuO NPs, *A. officinalis* extract and BHT. *$P<0.05$, **$P<0.01$, ***$P<0.001$ compared to BHT

Concentration (µg/mL)	DPPH-scavenging activity (%)		
	BHT	Extract	AO@CuO NPs
200	92.1±0.1	74.6±1.2***	73.0±2.4***
100	84.1±0.4	68.9±0.8***	64.3±0.5***
50	74.9±3.2	53.5±0.1***	40.0±0.3***
25	63.5±0.5	38.1±2.4***	23.5±2.2***
12.5	53.9±3.7	28.6±2.4***	19.1±1.2***

Determination of Cytotoxic Activity

DLD-1, A549, and HepG2 cells were used to evaluate cancer-fighting potential of AO@CuO NPs with different concentrations (0–250 µg/mL) using the MTT assay method. L929 cells were used for the toxicity test of AO@CuO NPs. Proliferation of DLD-1, A549, and HepG2 cells was inhibited dose-dependently by AO@CuO NPs. However, no significant decrease was observed in normal L929 cells. The IC_{50} values of A0@CuO NPs ranged from 10.7 to 253.9 µg/mL across tested cancer cell. These values are lower than those of the *A. officinalis* extract. This indicates that the AO@CuO nanoparticle formulation increases the cytotoxic effect. The results are shown in Table 6. Morphological changes induced by AO@CuO NPs were observed through the light inverted microscope, in contrast to the untreated control cells (Fig. 6). The cytotoxic profile of AO@CuO NPs is illustrated in Fig. 7. According to MTT results, AO@CuO NPs were most toxic to DLD-1 colorectal cancer cells. Additionally, cancer cells were more sensitive to the treatment compared to normal L929 fibroblast cells. Recently, Sathiyavimalu and colleagues have reported *Abutilon indicum* extract mediated green synthesis of CuO NPs has highly efficient antibacterial and anti-cancer properties against A549 and MDA-MB-231 cells. The IC_{50} values were determined as 16 µg/mL for A549 cells and 14 µg/mL for MDA-MB-231 cells, consistent with the results obtained in this study [62].

Table 6 The IC_{50} values of AO@CuO NPs and *A. officinalis* extract across all tested cancer cells

Cell Lines	IC_{50} values (µg/ml)	
	AO@CuO NPs	A. officinalis
A549	28.3±1.4	>250
DLD1	10.7±0.7	>250
HepG2	253.9±11.8	>250

The cytotoxic activity of CuO NPs synthesized using *Pimenta dioica* leaf extract was reported by Pillai and colleagues [63]. They examined antitumor activities against both human colorectal cancer and normal fibroblast cells. The IC_{50} value was found to be 89.42 µg/mL for the DLD-1 cell lines, demonstrating lower activity compared to our results. Their studies confirm that CuO NPs exhibit lower toxicity to normal fibroblast cells than to human colorectal cancer cells. Younas and colleagues reported the cytotoxic effects of CuO NPs against HepG2 cells induced by oxidative stress. At a concentration of 100 µg/mL, CuO NPs caused 46% decrease in the viability of hepatocellular carcinoma cells [64]. Recent studies have consistently shown that CuO NPs trigger ROS production in various cancer cell lines, leading to oxidative stress-mediated cytotoxicity [38, 65]. Moschini and colleagues examined the molecular mechanisms underlying CuO NPs–induced loss of cellular integrity and subsequent cell death in A549 cells. It has been determined that CuO NPs cause oxidative changes through increased protein carbonylation and decreased protein thiol oxidation [66].

Analysis of Apoptotic and Dead Cells by Muse Annexin V

The apoptotic induction of AO@CuO NPs and *A. officinalis* extract on DLD-1, A549, HepG2 and L929 cell lines was determined with flow cytometry analysis. Treatment with A0@CuO NPs induced an increase in apoptotic cells in DLD-1, A549, and HepG2 cells. Among the tested cell lines, AO@CuO NPs treatment resulted in the highest total apoptosis (early + late apoptosis) in A549 (55.5%) compared to 1.1% in control cells and DLD-1 cells (45%), compared to 2.0% in control cells (Fig. 8). The observed increase in apoptosis was consistent with the decrease in cell proliferation detected in the MTT assay. The flow cytometry plots are shown in Fig. 9. In comparison to the control group, AO@CuO NPs showed no significant effect on the proliferation of L929 cells. However, they were found to be effective in inducing apoptosis (43.2%). This phenomenon may likely be linked to the presence of a significant population of early apoptotic cells, which has not yet been reflected in

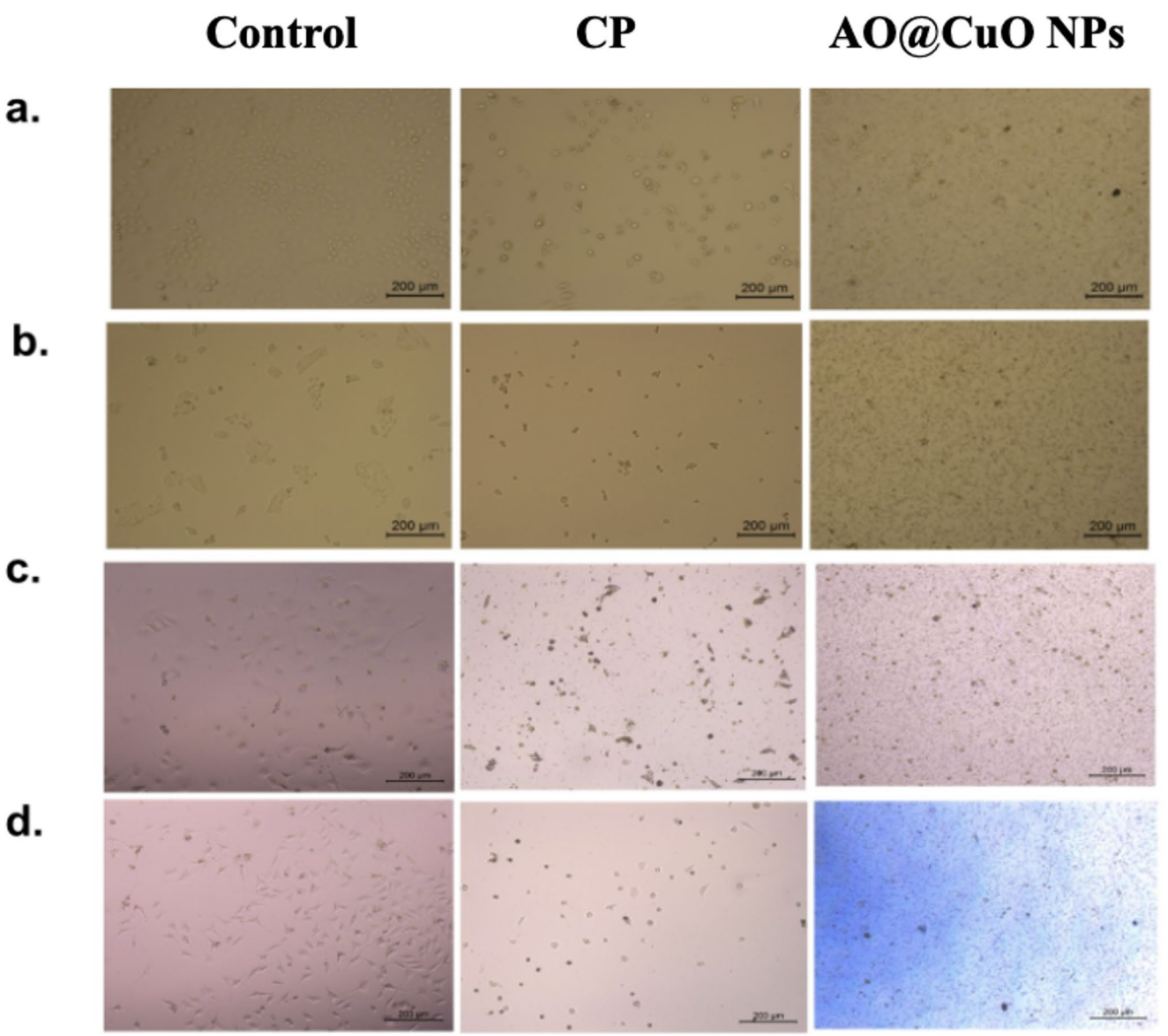


Fig. 6 Microscopic examination of CP and AO@CuO NPs against (**a**) A549, (**b**) DLD-1, (**c**) HepG2 and (**d**) L929 cells

proliferation. Conducting subsequent studies at later time points could potentially elucidate the impact of proliferation on the observed outcomes [67].

The intracellular ROS level and detailed molecular mechanism weren't directly assessed in the present study. Previous reports suggest that CuO NPs cause mitochondrial dysfunction and ROS production [68]. Increased oxidative stress can lead to disruption of mitochondrial membrane integrity, leakage of cytochrome C into the cytosol, and activation of the intrinsic apoptotic pathway [69]. Therefore, while the observed apoptotic effect may potentially be ROS-mediated, this should be confirmed by further molecular analysis. Increased ROS production can activate the caspase cascade (−3/9) [70], resulting in increased Bax expression and decreased Bcl-2 levels [71]. Farshori and colleagues, studies confirm that CuO NPs exhibit a dose-dependent cytotoxic profile on the HepG2 cell line. It has been demonstrated that CuO NPs also trigger the caspase cascade by disrupting mitochondrial homeostasis in HEp-2 cells. Furthermore, there were significant changes in mRNA transcription levels in Hep-2 cells. The activation of caspase-dependent pathways, particularly Bax, p53, and Bcl-2 factors, induced apoptosis [72]. Another study reported that CuO NPs showed cytotoxic effects on colorectal cancer cells (HCT-116), while causing minimal toxicity against normal healthy cells. The HCT-116 cell line was found to induce apoptosis by reducing Nrf-2 gene expression and increasing the expression of p53 genes and Bax [73]. According to Tennalli and colleagues, CuO NPs induced apoptosis in A549, MCF-7, and

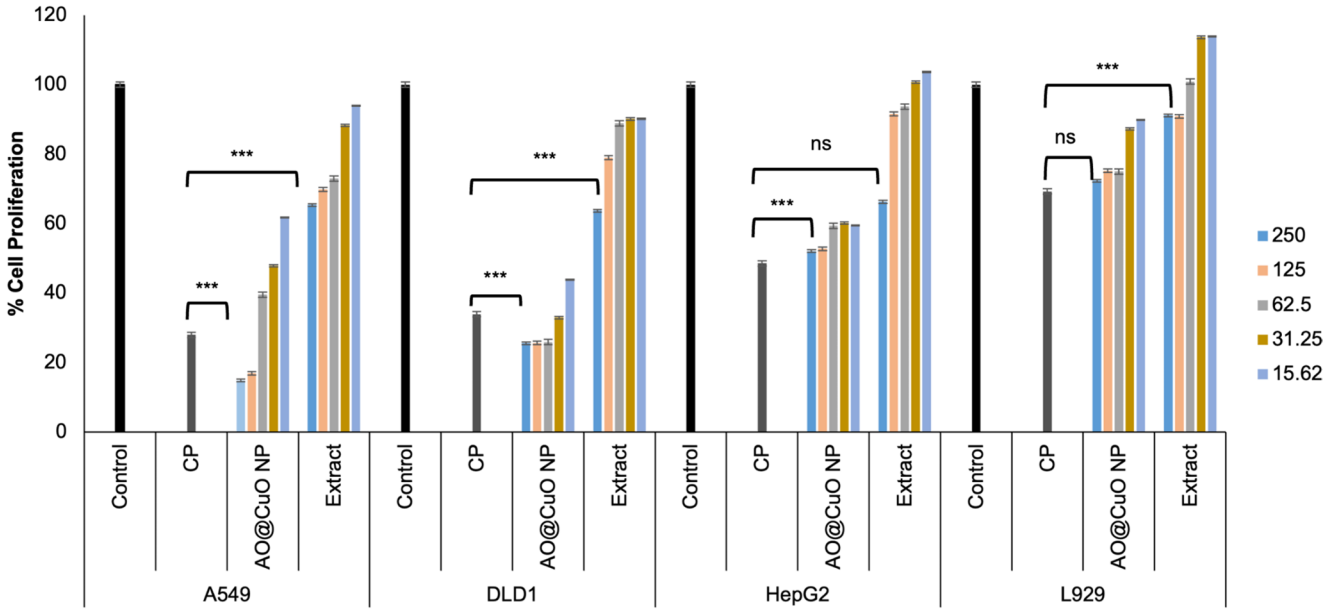


Fig. 7 Cell proliferation (%) of A549, DLD-1, HepG2 and L929 cells treated with AO@CuO NPs, *A. officinalis* extract and CP. The calculation was made by accepting the control group as 100%. Statistical significance was determined by comparing the highest concentrations of *A. officinalis* extract and AO@CuO NPs with CP (***:$P<0.001$, **:$P<0.0,1$ and *:$P<0.05$)

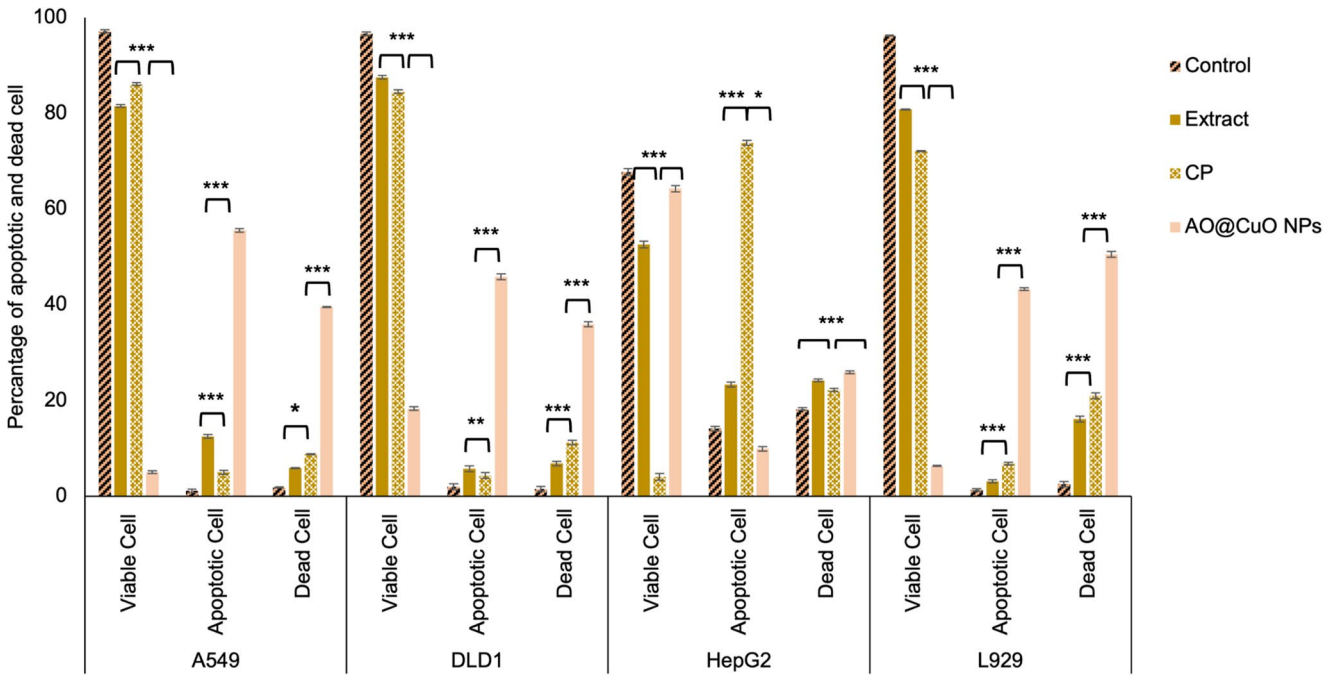


Fig. 8 Percentage of viable, apoptosis and dead cell in cell lines treated with IC_{50} values of AO@CuO NPs, *A. officinalis* extract and CP. Statistical significance was assessed by comparing percentages of *A. officinalis* extract and AO@CuO NPs with CP (***:$P<0.001$, **:$P<0.01$ and *:$P<0.05$)

HepG2 cells. The strongest effect observed in A-549 cells, consistent with our findings. Additionally, it has been suggested that the spherical nanostructure enhances surface reactivity and cellular uptake, thereby triggering apoptosis through increased ROS production, mitochondrial disruption, and DNA damage [74].

Conclusion

In this study, we report for the first time synthesis of CuO NPs using *A. officinalis* aqueous extract with a nature friendly, fast and low-cost green hydrothermal synthesis method. Characterization of AO@CuO NPs were

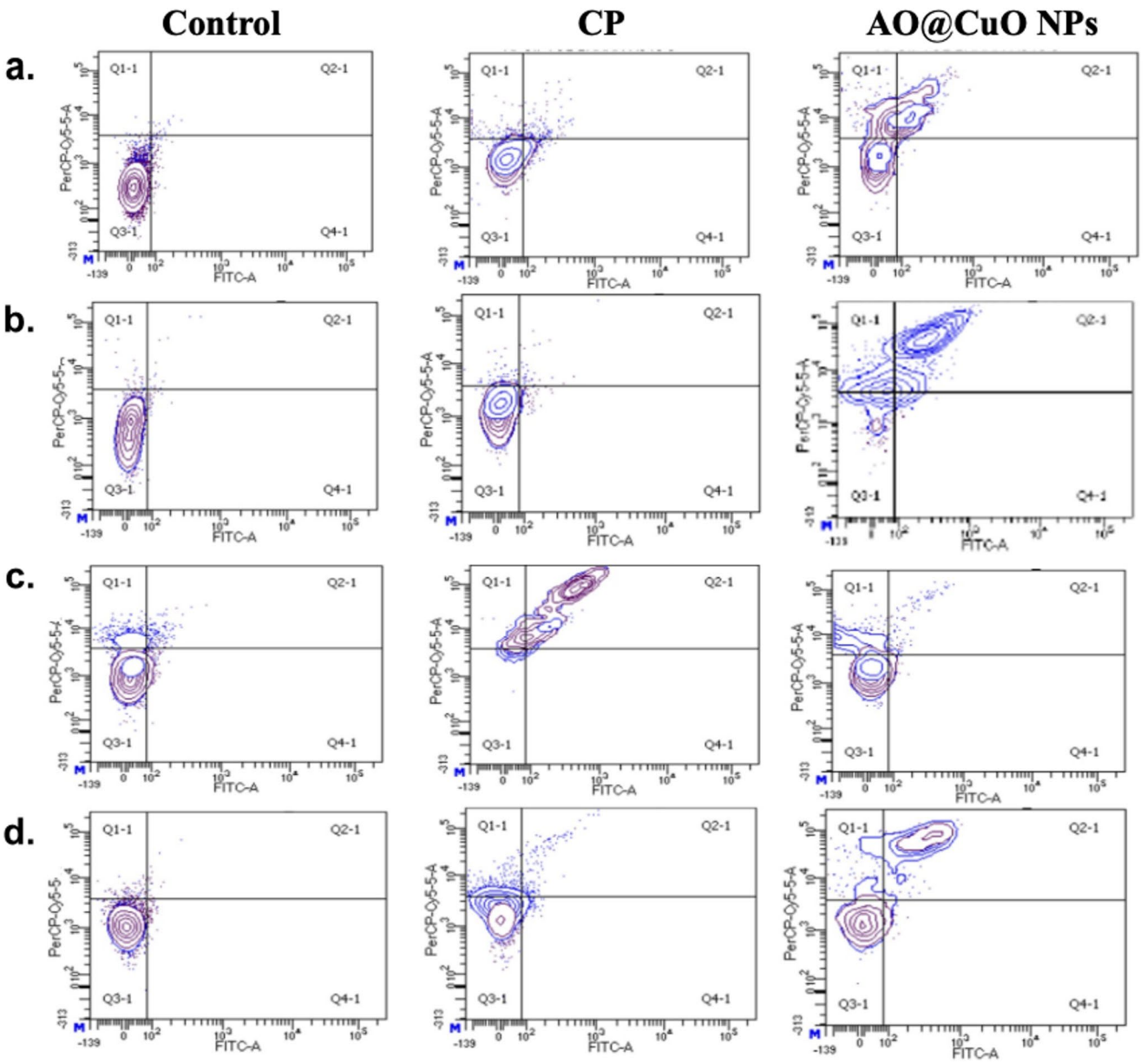


Fig. 9 Flow cytometry plots for apoptosis detection in (**a**) A549, (**b**) DLD-1, (**c**) HepG2, and (**d**) L929 cell lines. According to the flow chart, Q1 represents dead cells, Q2 late apoptotic cells, Q3 live cells, and Q4 early apoptotic cells

determined by UV-Vis spectroscopy, SEM, DLS, XRD, FT-IR and Zeta Potential. AO@CuO NPs were spherical structures with a mean diameter of 30 ± 10 nm. The FT-IR analysis indicates functional groups that play a significant role as the reducing and stabilizing for AO@CuO NPs. AO@CuO NPs demonstrated antibacterial, antibiofilm and antioxidant activity, making them potential candidates in various fields including healthcare, food industry and therapeutic applications. They showed in vitro cytotoxic and apoptosis-related activity in cancer cells. The apoptotic increase is observed in flow cytometry analysis, and the results are consistent with mechanisms described in the current scientific literature. However, to explain the molecular mechanism of CuO NPs fully, it is necessary to investigate molecular markers, such as ROS production, caspases-3/9 activities and Bax/Bcl-2 expression ratios. Following this biological investigation, future studies detailing these pathways will provide a strong foundation for various potential applications of AO@CuO NPs, such as biosensors and drug delivery systems.

Acknowledgements The authors thank the Scientific and Technological Research Council of Türkiye (TÜBITAK) with 1002-A Short-term Support Module, grant number 125Z252 for their financial support. Additionally, we would like to thank the Proofreading & Editing

Office of the Dean for Research at Erciyes University for the copyediting and proofreading service for this manuscript.

Author contributions EKD: Methodology, investigation, writing and review and editingCY and DB: İnvestigation, data curationSK: İnvestigation and validationİÖ: Supervision, writing, review and editingFÖK: Supervision, methodology, validation.

Funding Open access funding provided by the Scientific and Technological Research Council of Türkiye (TÜBİTAK). This research was funded by the Scientific and Technological Research Council of Türkiye (TÜBITAK) with 1002-A Short-term Support Module (under Grant Number 125Z252).

Data Availability The data that support the findings of this study are available from the corresponding author upon reasonable request. However, due to privacy and project restrictions, the datasets are not publicly available.

Declarations

Competing interests The authors declare no competing interests.

Open Access This article is licensed under a Creative Commons Attribution 4.0 International License, which permits use, sharing, adaptation, distribution and reproduction in any medium or format, as long as you give appropriate credit to the original author(s) and the source, provide a link to the Creative Commons licence, and indicate if changes were made. The images or other third party material in this article are included in the article's Creative Commons licence, unless indicated otherwise in a credit line to the material. If material is not included in the article's Creative Commons licence and your intended use is not permitted by statutory regulation or exceeds the permitted use, you will need to obtain permission directly from the copyright holder. To view a copy of this licence, visit http://creativecommons.org/licenses/by/4.0/.

References

1. M. Parmar, & M. Sanyal, Extensive study on plant mediated green synthesis of metal nanoparticles and their application for degradation of cationic and anionic dyes, *Environmental Nanotechnology, Monitoring & Management*, *17*, 100624, (2022) https://doi.org/10.1016/j.enmm.2021.100624
2. S. Vijayaram, H. Razafindralambo, Y. Z. Sun, S. Vasantharaj, H. Ghafarifarsani, S. H. Hoseinifar, & M. Raeeszadeh, Applications of green synthesized metal nanoparticles—a review, *Biological Trace Element Research*, *202*(1), 360–386, (2024) https://doi.org/10.1007/s12011-023-03645-9
3. S. Salavati, & M. Kakaei, Investigating the biochemical characteristics of different species of the medicinal plant of Marshmallow (Althaea L.), *Ecophytochemistry Journal of Medicinal Plants*, *12*(4), 83–100, (2025)
4. N. Pryvedeniuk, L. Hlushchenko, A. Sereda, A. Shatkovskyi, O. Zhuravlov, L. Mishchenko, & I. Mishchenko, Features of polysaccharide accumulation in Althaea officinalis L. raw material under various technological methods, *International Journal of Secondary Metabolite*, (Advanced Online Publication), 23–35,(2026) https://doi.org/10.21448/ijsm.1669512
5. M. A. Kalam, R. Ahmad, M. Avid, A. Rahim, & A Habib, Khatmī (Althea officinalis L. and Althea rosea): Medicinal importance in the perspective of Unani medicine and pharmacological studies, *Journal of Drug Delivery & Therapeutics*, *13*(12), 270–277,(2023) https://doi.org/10.53390/ijum.2024.17212
6. C. Farhat, H. Younes, O. Alyamani, M. Mrad, N. Hourani, H. Khalifeh, & R. Hage-Sleiman, Chemical characterization and in vitro biological evaluation of aqueous extract of Althaea officinalis L. flower grown in Lebanon, *Journal of Herbal Medicine*, *34*, 100575, (2022) https://doi.org/10.1016/j.hermed.2022.100575
7. M. Wang, J. Pan, W. Xiang, Z. You, Y. Zhang, J. Wang, & A. Zhang, β-glucan: A potent adjuvant in immunotherapy for digestive tract tumors, *Frontiers in Immunology*, *15*, 1424261, (2024) https://doi.org/10.3389/fimmu.2024.1424261
8. V. Vetvicka, & J. Vetvickova, Anti-infectious and anti-tumor activities of β-glucans, *Anticancer Research*, *40*(6), 3139–3145, (2020) https://doi.org/10.21873/anticanres.14295
9. A. Turgumbayeva, B. Baimakhanova, A. Sadanov, I. Ratnikova, S. Orasymbet, E. Shorabaev, & A. Zhalgaskali, Phytochemical compounds and biomedical properties of Althaea officinalis, *Pharmacy Practice*, *23*(3), 1–15, (2025) https://doi.org/10.18549/pharmpract.2025.3.3153
10. M. Arab, N. Arab, D. Kahrizi, & A. G. Ebadi, Evaluating Antibacterial Effects of Alcoholic Extracts and Essential Oil of Althaea officinalis Against Two Types of Gram-positive and Gram-negative Bacteria (Bacillus cereus and Klebsiella pneumonia), *Journal of Medicinal Plants & By-Products*, *12*(1), (2023)
11. D. T. Rheder, M. Guilger, N. Bilesky-José, T. Germano-Costa, T. Pasquoto-Stigliani, T. B. B. Gallep, …R. Lima, Synthesis of biogenic silver nanoparticles using Althaea officinalis as reducing agent: evaluation of toxicity and ecotoxicity, *Scientific reports*, *8*(1), 12397, (2018) https://doi.org/10.1038/s41598-018-30317-9
12. A. L. Jafari, K. Pourakbar, L. Farhadi, M. GHOLIZAD, & Y. Goosta, Biological synthesis of silver nanoparticles and evaluation of antibacterial and antifungal properties of silver and copper nanoparticles, *Turkish Journal of Biology*, *39*(4), 556–561, (2015) https://doi.org/10.3906/biy-1406-81
13. H. Korbekandi, G. Asghari, M. R. Chitsazi, R. Bahri Najafi, A. Badii, & S. Iravani, Green biosynthesis of silver nanoparticles using Althaea officinalis radix hydroalcoholic extract, *Artificial cells, nanomedicine, and biotechnology*, *44*(1), 209–215,(2016) https://doi.org/10.3109/21691401.2014.936064
14. S. F. Elhabal, N. Abdelaal, S. A. K. Saeed Al-Zuhairy, M. F. M. Elrefai, A. M. Elsaid Hamdan, M. M. Khalifa, …M. A. El-Nabarawi, Green synthesis of zinc oxide nanoparticles from Althaea officinalis flower extract coated with chitosan for potential healing effects on diabetic wounds by inhibiting TNF-α and IL-6/IL-1β signalling pathways, *International Journal of Nanomedicine*, 3045–3070, (2024) https://doi.org/10.2147/ijn.s455270
15. X. Ma, S. Zhou, X. Xu, Q. Du, Copper-containing nanoparticles: Mechanism of antimicrobial effect and application in dentistry-a narrative review, *Frontiers in surgery*, *9*, 905892, (2022) https://doi.org/10.3389/fsurg.2022.905892
16. L. R. Milam, & R. P. Planalp, Bimetallic Fenton-like catalysts in the remediation of dyes, *Colorants*, *3*(1), 1–16, (2023)
17. S. Naz, A. Gul, M. Zia, & R. Javed, Synthesis, biomedical applications, and toxicity of CuO nanoparticles, *Applied Microbiology and Biotechnology*, *107*(4), 1039–1061, (2023) https://doi.org/10.1007/s00253-023-12364-z
18. M. Ramzam, R. M. Obodo, S. Mukhtar, S. Z. Ilyas, F. Aziz, & N Thovhogi, Green synthesis of copper oxide nanoparticles using Cedrus deodara aqueous extract for antibacterial activity. *Materials Today: Proceedings*, *36*, 576–581, (2021,https://doi.org/10.1016/j.matpr.2020.05.472
19. N. Kütük, & S. Çetinkaya, Green synthesis of copper oxide nanoparticles using black, green and tarragon tea and investigation

of their photocatalytic activity for methylene blue, *Pamukkale Üniversitesi Mühendislik Bilimleri Dergisi*, *28*(7),, 955–962, (2022) https://doi.org/10.5505/pajes.2022.47037
20. N. Ghasemi, F. Jamali-Sheini, R. Zekavati, CuO and Ag/CuO nanoparticles: Biosynthesis and antibacterial properties, Mater. Lett. 1 (196), 78–82, (2017) https://doi.org/10.1016/j.matlet.2017.02.111
21. M. Kouhkan, P. Ahangar, L. A. Babaganjeh, M. Allahyari-Devin, Biosynthesis of copper oxide nanoparticles using Lactobacillus casei subsp. casei and its anticancer and antibacterial activities, Curr. Nanosci, 16(1), 101–11, (2020), https://doi.org/10.2174/1573413715666190318155801
22. S. A. Akintelu, A. S. Folorunso, F. A. Folorunso, A. K. Oyebamiji, Green synthesis of copper oxide nanoparticles for biomedical application and environmental remediation, Heliyon, 6 (7), e04508, (2020) https://doi.org/10.1016/j.heliyon.2020.e04508 .
23. B. Murugan, M. Z. Rahman, I. Fatimah, J. A. Lett, J Annaraj, N. H. M. Kaus, & S. Sagadevan, Green synthesis of CuO nanoparticles for biological applications, *Inorganic Chemistry Communications*, *155*, 111088, (2023) https://doi.org/10.1016/j.inoche.2023.111088.
24. S. Dhir, R. Dutt, R. P. Singh, M. Chauhan, T. Virmani, G. Kumar, … M. Al-Zahrani,Amomum subulatum fruit extract mediated green synthesis of silver and copper oxide nanoparticles: synthesis, characterization, antibacterial and anticancer activities,*Processes*, *11*(9), 2698, (2023) https://doi.org/10.3390/pr11092698
25. P. Prabu, & V. Losetty, Green synthesis of copper oxide nanoparticles using Macroptilium Lathyroides (L) leaf extract and their spectroscopic characterization, biological activity and photocatalytic dye degradation study, *Journal of Molecular Structure*, *1301*, 137404, (2024) https://doi.org/10.1016/j.molstruc.2023.137404
26. T. A. Zughaibi, A. A. Mirza, M. Suhail, N. R. Jabir, S. K. Zaidi, S. Wasi, … S. Tabrez,Evaluation of anticancer potential of biogenic copper oxide nanoparticles (CuO NPs)against breast cancer, *Journal of Nanomaterials*, 1–7, (2022) https://doi.org/10.1155/2022/5326355
27. R. Manivannan, G. S. Kumar, D. Kamalakannan, V. H. Deventhiran, P. R. Rajsekar, V. Senthilkumar, & M. Shivaganesh, Green synthesis of Tecoma stans leaves-mediated copper oxide nanoparticles: Preparation, antioxidant, antimicrobial activities and in vitro MTT assay against MG-63 cell line, *Journal of Pharmacognosy and Phytochemistry*, *12*(3),195–201, (2023).
28. F. Ö. Küp, S. Çoşkunçay, & F. Duman, Biosynthesis of silver nanoparticles using leaf extract of Aesculus hippocastanum (horse chestnut): Evaluation of their antibacterial, antioxidant and drug release system activities, Materials Science and Engineering: C, 107, 110207, (2020) https://doi.org/10.1016/j.msec.2019.110207
29. K. ur. Rehman, A. U. Khan, K. Tahir, S. Nazir, K. Albalawi, H. M. Hassan, … A. M.Aldawsari, Facile synthesis of copper oxide nanoparticles (CuONPs) using green method to promote photocatalytic and biocidal applications, *Journal of Molecular Liquids*, *360*, 119453, (2022) https://doi.org/10.1016/j.molliq.2022.119453
30. S. T. Parveen, & K. Riazunnisa, Phytofabrication of copper nanoparticles using Momordica cymbalaria fruit extract and their antibacterial, antioxidant and anti-inflammatory properties, *Hybrid Advances*, *9*, 10042, (2025) https://doi.org/10.1016/j.hybadv.2025.100421
31. A. M. Shehabeldine, B. H. Amin, F. A. Hagras, A. A. Ramadan, M. R. Kamel, M. A. Ahmed, & S. S. Salem, Potential antimicrobial and antibiofilm properties of copper oxide nanoparticles: time-kill kinetic essay and ultrastructure of pathogenic bacterial cells, *Applied Biochemistry and Biotechnology*, *195*(1), 467–485, (2023) https://doi.org/10.1007/s12010-022-04120-2
32. S. V. Gudkov, D. E. Burmistrov, P. A. Fomina, S. Z. Validov, & V. A. Kozlov, Antibacterial properties of copper oxide nanoparticles, *International Journal of Molecular Sciences*, *25*(21), 11563, (2024) https://doi.org/10.3390/ijms252111563
33. U. Rajchakit, S. Lamba, K. Wang, N. Lyons, J. Lu, S. Swift, … V. Sarojini, Size-controlled synthesis of gold nanoparticles tethering antimicrobial peptides with potent broad-spectrum antimicrobial and antibiofilm activities,*Molecular Pharmaceutics*, 21(2), 596–608, (2024) https://doi.org/10.1021/acs.molpharmaceut.3c00734
34. A. S. Aliero, N. A. Zawawi, N. A. N. N. Malek, M. H. Sani, M. H. Asraf, S. W. To,… A. Haruna, Biocompatible antibacterial and antibiofilm activities of silver nanoparticles synthesized using palm oil mill effluent, *Biomass Conversion and Biorefinery*, 1–14 (2024)https://doi.org/10.1007/s13399-024-06405-4
35. T. Khairy, D. H. Amin, H. M. Salama, I. M. A. Elkholy, M. Elnakib, H. M. Gebreel, & H. A. E. Sayed, Antibacterial activity of green synthesized copper oxide nanoparticles against multidrug-resistant bacteria, Scientific Reports, 14(1), 25020, (2024) https://doi.org/10.1038/s41598-024-75147-0
36. F. Duman, I. Ocsoy, & F. O. Kup, Chamomile flower extract-directed CuO nanoparticle formation for its antioxidant and DNA cleavage properties, Materials Science and Engineering:C, 60, 333–338, (2016) https://doi.org/10.1016/j.msec.2015.11.052
37. S. Mani, & G. Swargiary, In vitro cytotoxicity analysis: MTT/XTT, trypan blue exclusion. In *Animal cell culture: principles and practice* (pp. 267–284), Cham: Springer International Publishing, 267–284, (2023) https://doi.org/10.1007/978-3-031-19485-6_18
38. M. Dolati, F. Tafvizi, M. Salehipour, T. Komeili Movahed, & P. Jafari, Biogenic copper oxide nanoparticles from Bacillus coagulans induced reactive oxygen species generation and apoptotic and anti-metastatic activities in breast cancer cells, *Scientific Reports*, *13*(1), 3256, (2023) https://doi.org/10.1038/s41598-023-30436-y
39. S. Annathurai, S. Chidambaram, B. Baskaran, & G. K. Prasanna Venkatesan, Green synthesis and electrical properties of p-CuO/n-ZnO heterojunction diodes, *Journal of Inorganic and Organometallic Polymers and Materials*, *29*, 535–540, (2019) https://doi.org/10.1007/s10904-018-1026-1
40. S. Latif, F. Abdulaziz, A. M. Alanazi, A. H. Alsehli, M. M. Alsowayigh, & A. A Alanazi, Effect of H2O2@ CuONPs in the UV light-induced removal of organic pollutant Congo red dye: investigation into mechanism with additional biomedical study, *Molecules*, *28*(1), 410, (2023) https://doi.org/10.3390/molecules28010410
41. A. K. Zak, W. A. Majid, M. R. Mahmoudian, M. Darroudi, & R. Yousefi, Starch- stabilized synthesis of ZnO nanopowders at low temperature and optical properties study, *Advanced Powder Technology*, *24*(3), 618 624, (2013) https://doi.org/10.1016/j.apt.2012.11.008
42. M. J. Javid-Naderi, Z. Sabouri, A. Jalili, H. Zarrinfar, S. Samarghandian, & M. Darroudi, Green synthesis of copper oxide nanoparticles using okra (Abelmoschus esculentus) fruit extract and assessment of their cytotoxicity and photocatalytic applications, *Environmental Technology & Innovation*, *32*, 103300, (2023) https://doi.org/10.1016/j.eti.2023.103300
43. J. D. O. Primo, C. Bittencourt, S. Acosta, A. Sierra-Castillo, F. J. Colomer, S. Jaerger,… F. J. Anaissi, Synthesis of zinc oxide nanoparticles by ecofriendly routes: adsorbent for copper removal from wastewater, *Frontiers in Chemistry*, *8*, 571790, (2020) https://doi.org/10.3389/fchem.2020.571790
44. Z. Németh, I. Csóka, R. Semnani Jazani, B. Sipos, H. Haspel, G. Kozma, & D. G. Dobó, Quality by design-driven zeta potential optimisation study of liposomes with charge imparting membrane

additives, *Pharmaceutics*, *14*(9), 1798, (2022) https://doi.org/10.3390/pharmaceutics14091798
45. J. N. Meegoda, S. A. Hewage, & J. H. Batagoda, Application of the diffused double layer theory to nanobubbles, *Langmuir*, 35(37), 12100–12112, (2019) https://doi.org/10.1021/acs.langmuir.9b01443
46. S. Bhattacharjee, DLS and zeta potential–what they are and what they are not? *Journal of controlled release*, 235, 337–351, (2016) https://doi.org/10.1016/j.jconrel.2016.06.017
47. N. T. Anh, N. X. Dinh, H. Van Tuan, T. H. Thuan, L. M. Tung, V. P. Le, … A. T. Le,Cost-Effective Tween 80-Capped Copper Nanoparticles for Ultrasensitive Colorimetric Detection of Thiram Pesticide in Environmental Water Samples, *Journal of Nanomaterials*, 5513401,(2021) https://doi.org/10.1155/2021/5513401
48. V. Sudha, G. Murugadoss, & R. Thangamuthu, Structural and morphological tuning of Cu-based metal oxide nanoparticles by a facile chemical method and highly electrochemical sensing of sulphite, Scientific reports, 11(1), 3413, (2021) https://doi.org/10.1038/s41598-021-82741-z
49. D. Khidhir, & H. Sidiq, Efficacy of green oxide nanofluids as potential dispersants for asphaltene in Iraqi crudes, experimental, tunning and statistical analysis. *Energies*, *15*(18), 6833, (2022).
50. S. Pasieczna-Patkowska, M. Cichy, & J. Flieger, Application of Fourier transform infrared (FTIR) spectroscopy in characterization of green synthesized nanoparticles, *Molecules*, *30*(3), 684, (2025) https://doi.org/10.3390/molecules30030684
51. K. Ganesan, V. Jothi, A. Natarajan, A. Rajaram, S. Ravichandran, S. Ramalingam, Green synthesis of copper oxide nanoparticles decorated with graphene oxide for anticancer activity and catalytic applications, *Arabian Journal of Chemistry*, *13*(*8*), 6802–6814, (2020) https://doi.org/10.1016/j.arabjc.2020.06.033
52. D. Franco, G. Calabrese, S. P. P. Guglielmino, & S. Conoci, Metal-based nanoparticles: antibacterial mechanisms and biomedical application, *Microorganisms*, *10*(9), 1778,(2022) https://doi.org/10.3390/microorganisms10091778
53. K. Riazunnisa, M. S. V. Narayana, N. Rajesh, M. Kiranmayee, Phytosynthesis of Copper Oxide Nanoparticles From Pithecellobium dulce: A Synergy of Experimental and In Silico Analysis for Biomedical Potential, *Chemistry & Biodiversity*, *22*(12), e00998, (2025) https://doi.org/10.1002/cbdv.202500998
54. A. R. Padmavathi, A. Das, A. Priya, T. J. Sushmitha, S. K. Pandian, & S. R. Toleti, Impediment to growth and yeast-to-hyphae transition in Candida albicans by copper oxide nanoparticles, *Biofouling*, *36*(1), 56–72, (2020) https://doi.org/10.1080/08927014.2020.1715371
55. G. Mi, D. Shi, M. Wang, & T. J. Webster, Reducing bacterial infections and biofilm formation using nanoparticles and nanostructured antibacterial surfaces, Advanced Healthcare Materials, 7(13), 1800103, (2018) https://doi.org/10.1002/adhm.201800103
56. X. Zhu, D. Liu, A. K. Singh, R. Drolia, X. Bai, S. Tenguria, & A. K. Bhunia, Tunicamycin mediated inhibition of wall teichoic acid affects Staphylococcus aureus and Listeria monocytogenes cell morphology, biofilm formation and virulence, *Frontiers in microbiology*, *9*, 1352, (2018) https://doi.org/10.3389/fmicb.2018.01352
57. M. Mirzaee, S. N. Peerayeh & A. Ghasemian, Detection of icaABCD genes and biofilm formation in clinical isolates of methicillin resistant Staphylococcus aureus, Iranian Journal of Pathology, 9, 257–262, (2014)
58. R. G. Daré, & S. O. Lautenschlager, Nanoparticles with antioxidant activity. *Antioxidants*, *14*(2), 221, (2025) https://doi.org/10.3390/antiox14020221
59. M. Martínez-Cabanas, M. López-García, P. Rodríguez-Barro,T. Vilariño, P. Lodeiro, R. Herrero, & M. E. Sastre de Vicente, Antioxidant capacity assessment of plant extracts for green synthesis of nanoparticles. *Nanomaterials*, *11*(7), 1679, (2021) https://doi.org/10.3390/nano11071679
60. S. M. Azharuddin, C. Madhuri, N. Rajesh, K. Riazunnisa, Sustainable phycosynthesis of copper oxide nanoparticles from Arthospira platensis: Synergistic computational and experimental bioactivity evaluation, *Journal of Environmental Chemical Engineering*, 121013, (2026) https://doi.org/10.1016/j.jece.2025.121013
61. M. S. V. Narayana, N. Rajesh, C. Dastagiri, S. A. Mobeen, H. Khadri, T. Chandrasekhar, & K. Riazunnisa, Pleurotus ostreatus copper nanoparticles: in vitro and in Silico evaluation of the antioxidant, antibacterial, and antidiabetic activities, *Chemistry & Biodiversity*, *22*(5), e20240236, (2025) https://doi.org/10.1002/cbdv.202402361
62. S. Sathiyavimal, E. F. Durán-Lara, S. Vasantharaj, M. Saravanan, A. Sabour, M. Alshiekheid,… A. Pugazhendhi, Green synthesis of copper oxide nanoparticles using Abutilon indicum leaves extract and their evaluation of antibacterial, anticancer in human A549 lung and MDA-MB-231 breast cancer cells, Food and Chemical Toxicology, 168, 113330, (2022)https://doi.org/10.1016/j.fct.2022.113330
63. R. R. Pillai, P. B. Sreelekshmi, & A. P. Meera, Enhanced biological performance of green synthesized copper oxide nanoparticles using Pimenta dioica leaf extract, *Materials Today: Proceedings*, *50*, 163–172, (2022) https://doi.org/10.1016/j.matpr.2021.11.547
64. M. Younas, M. Zubair, M. Rizwan, M. A. Khan, K. M. Hussaini, R. Mumtaz, & S. Ali, Synthesis and characterization of cerium, silver and copper oxide nanoparticles and their anticancer potential of hepatocellular carcinoma HepG2 cancer cells, *Journal of Molecular Structure*, *1288*, 135756, (2023) https://doi.org/10.1016/j.molstruc.2023.135756.
65. M. Sakthivel, K. Vimala, M. Rajkumar, S. Navaneethakrishnan, R. Thangaraj, & S. Kannan, Fabrication of Biosynthesis CuO Nanoparticles Mediated by Artemisia vulgaris: A Novel Target for Colon Cancer Therapy Via Suppression of PI3K/AKT/mTOR Signaling Pathway. *Journal of Cluster Science*, *36*(6), 221, (2025) https://doi.org/10.1007/s10876-025-02944-6.
66. E. Moschini, G. Colombo, G. Chirico, G. Capitani, I Dalle-Donne, & P. Mantecca, Biological mechanism of cell oxidative stress and death during short-term exposure to nano CuO, *Scientific reports*, *13*(1), 2326, (2023) https://doi.org/10.1038/s41598-023-28958-6.
67. K. S. Shekhawat, P. Bhatia, K. Bhatnagar, S. Shandilay, & S. Chaudhary, Roadmap to cytotoxicity: exploring assays and mechanism,. *ASSAY and Drug Development Technologies*, *23*(5), 217–236, (2025) https://doi.org/10.1089/adt.2024.109.
68. M. M. Khalifa, & N. A. Hussien, Anticancer and anti-inflammatory potentials of doped CuO and ZnO nanoparticles: a multipathway mechanistic study, *Open Chemistry*, *24*(1), 20250225, (2026) https://doi.org/10.1515/chem-2025-0225
69. Y Shi, A R Pilozzi,& X Huang, Exposure of CuO nanoparticles contributes to cellular apoptosis, redox stress, and Alzheimer's Aβ amyloidosis, *International Journal of Environmental Research and Public Health*, *17*(3), 1005, (2020) https://doi.org/10.3390/ijerph17031005
70. R I Mahmood, A A Kadhim, S Ibraheem, S Albukhaty, H S Mohammed-Salih, R H Abbas, & H Al-Karagoly, Biosynthesis of copper oxide nanoparticles mediated Annona muricata as cytotoxic and apoptosis inducer factor in breast cancer cell lines, *Scientific Reports*, *12*(1), 16165, (2022) https://doi.org/10.1038/s41598-022-20360-y
71. S Seghatoleslami, M Pourmohammad, H Mahmoudzadeh, & J Khayatzadeh, Augmenting the cytotoxicity and apoptosis induction of green synthesized copper oxide nanoparticles from Artemisia sieberi by combining with tamoxifen: Mechanism involving Bax/Bcl-2 modulation, *Journal of Pharmaceutical Sciences*, 104143, (2025) https://doi.org/10.1016/j.xphs.2025.104143

72. N. N. Farshori, M. A. Siddiqui, M. M. Al-Oqail, E. S. Al-Sheddi, S. M. Al-Massarani, M. Ahamed, & A. A. Al-Khedhairy, Copper oxide nanoparticles exhibit cell death through oxidative stress responses in human airway epithelial cells: a mechanistic study, *Biological trace element research*, *200*(12), 5042–5051, (2022) https://doi.org/10.1007/s12011-022-03107-8 .
73. H. Abdollahzadeh, Y. Pazhang, A. Zamani, & Y. Sharafi, Green synthesis of copper oxide nanoparticles using walnut shell and their size dependent anticancer effects on breast and colorectal cancer cell lines, *Scientific Reports*, *14*(1), 20323, (2024) https://doi.org/10.1038/s41598-024-71234-4 .
74. G. B. Tennalli, S. Yallappa, B. S. Hungund, S. Joseph, M. N. Divate, & K. Upadhyaya, Biogenic synthesis of copper oxide nanoparticles from Ricinus communis L. leaf extract and their cytotoxic and pro-apoptotic effects on tumor cell lines, *Results in Chemistry*, 102896, (2025) https://doi.org/10.1016/j.rechem.2025.102896 .

Publisher's Note Springer Nature remains neutral with regard to jurisdictional claims in published maps and institutional affiliations.